Zero-dimensional transient model of large-scale cooling ponds using well-mixed approach

Ahmed Ramadan[1]*, Reaz Hasan[2], Roger Penlington[3]

[1, 2, 3] Northumbria University at Newcastle, Department of Mechanical and Construction Engineering, Newcastle upon Tyne, NE1 8ST, UK.

* corresponding author: Ahmed Ramadan: Fax: +44 191 232 6002 E-mail address: ahmed.ramadan@northumbria.ac.uk

Abstract

Nowadays, nuclear power plants around the world produce vast amounts of spent fuel. After discharge, it requires adequate cooling to prevent radioactive materials being released into the environment. One of the systems available to provide such cooling is the spent fuel cooling pond. The recent incident at Fukushima, Japan shows that these cooling ponds are associated with safety concerns and scientific studies are required to analyse their thermal performance. However, the modelling of spent fuel cooling ponds can be very challenging. Due to their large size and the complex phenomena of heat and mass transfer involved in such systems. In the present study, we have developed a zero-dimensional (Z-D) model based on the well-mixed approach for a large-scale cooling pond. This model requires low computational time compared with other methods such as computational fluid dynamics (CFD) but gives reasonable results are key performance data. This Z-D model takes into account the heat transfer processes taking place within the water body and the volume of humid air above its surface as well as the ventilation system. The methodology of the Z-D model was validated against data collected from existing cooling ponds. A number of studies are conducted considering normal operating conditions as well as in a loss of cooling scenario. Moreover, a discussion of the implications of the assumption to neglect heat loss from the water surface in the context of large-scale ponds is also presented. Also, a sensitivity study is performed to examine the effect of weather conditions on pond performance.

Keywords: Spent nuclear fuel, large-scale cooling ponds, analytical modelling, well-mixed approach, transient heat transfer.

Nomenclature

A	surface area (m^2)
C_p	specific heat capacity at constant pressure (J/kg K)
C_w	specific heat capacity of water (J/kg K)
h_c	convection heat transfer coefficient (W/m^2 K)
h_{con}	condensation mass transfer coefficient (m/s)
h_{ev}	evaporation mass transfer coefficient (m/s)
$h_v(T)$	enthalpy of vapour at a given temperature (kJ/kg)
h_{fg}	latent heat of vaporisation for water (kJ/kg)
k	thermal conductivity (W/m K)
m	mass (kg)
$\dot{m}$	mass flow rate (kg/s)
M	molecular weight (kg/kmol)
N	mole number (kmol)
$\dot{N}$	molar flow rate (kmol/s)
Nu	Nusselt number
P	pressure (Pa)
$\dot{Q}$	heat transfer rate (W)
Ra	Rayleigh number
RH	relative humidity (%)
R_o	universal gas constant (J/K kmol)
Sh	Sherwood number
T	temperature (K)
V	Volume (m^3)
x	wall thickness (m)
y	mole fractions
Δt	time step size (s)

Greek symbols

ε	emissivity
ρ	density (kg/m^3)
σ	Stefan-Boltzmann constant ($W/m^2 K^4$)

Subscripts

a	dry air
∞	ambient
c	convection
con	condensation
d	heat load
D	designed value
ev	Evaporation
h	hall
l	leakage
m	make-up
p	pond
r	radiation
R	rack
sat	saturation
t	total
v	vapour
$vent$	ventilation
w	water
wb	wet bulb

1 Introduction

In the past decades, increasing the use of nuclear power for electricity generation has gained a lot of attention amongst scientists. Nuclear reactors around the world are now discharging a massive amount of spent nuclear fuel, which is predicted to reach approximately 445,000 t HM (metric tonnes of heavy metal) by 2020 [1]. This includes 69,000 t in Europe and 60,000 t in North America. Despite the recent incident at Fukushima, Japan [2], nuclear power generation continue to grow in developed countries, as evidenced by the recent massive investment in nuclear energy by the UK government in approving an £18bn nuclear plant at Hinkley Point C. This will deliver 7% of Britain's electricity needs for the next six decades [3].

The issue of long-term storage was not considered when the original decisions were made regarding the fuel cycle [4]. Recently, waste management has become one of the major policy issues in most nuclear power programmes. Meanwhile, the options chosen for waste management can have extensive effects on political debates, propagation risks, environmental threats, and economic costs of the nuclear fuel cycle. This increases the significance of modelling the cooling ponds and analysing their performance to provide a better understanding of their pond thermal behaviour. This will allow for better operation and could offer mitigation options whenever needed in accident scenarios.

Several research investigations have considered the thermal-hydraulic behaviour of the spent fuel cooling ponds, which are mainly focused on accident scenarios and their consequences [2, 5-8]. These studies used two main modelling approaches. The first approach is the use of so-called system codes such as RELAP, TRACE, ATHLET, MELCOR and ASTEC. These codes are based on dividing the system into a network of pipes, pumps, vessels, and heat exchangers. Mass, momentum and energy conservation equations are then solved in one-dimensional form. Many phenomena and physical behaviour such as two-phase flows and pressure drop due to friction rely on empirical correlations. These codes are suitable for systems that can be represented by one-dimensional flows. However, when such a system involves multi-dimensional phenomena, these codes do not provide a good approximation. Some attempts have been made to improve their capability to handle multi-dimensional flows. One of these attempts considers the system as an array of parallel one-dimensional pipes, where the interaction between them is allowed through cross-flow coupling. Although they provide improved approximations compared with purely one-dimensional approaches, these models do

not offer appropriate descriptions of multi-dimensional flows. The MARS code is an example of attempts to include a multi-dimensional analysis capability in system codes [9].

The second approach is a numerical method such as computational fluid dynamics (CFD) which in principle can address details of thermos-fluid phenomena in cooling ponds Numerical methods such as CFD can be used, in principle, to address fluid flow and heat transfer scenarios in three dimensions using computers. The CFD methodology is now well-established, but the available literature indicates that a full CFD model of a spent fuel cooling pond may be not practically possible. This is due to their large size and the existence of complex phenomena, such as evaporation, which requires multiphase flow models. However, some studies have reported CFD modelling of spent fuel ponds taking into account only the water body without considering the humid air zone above or ventilation and their effect on the evaporation rate. Also, some of the challenges encountered during the CFD simulation have been discussed in our previous work [10]. An example of the use of CFD in improving the safety of such cooling ponds can be found in a study conducted by Ye et al. [11], in which a new passive cooling system was designed to provide an adequate cooling for the CAP1400 spent fuel pool in emergency situations. Hung et al. [12] used the CFD approach to predict the cooling ability of the Kuosheng spent fuel pool and to confirm that the existing configuration can provide enough cooling to meet licensing regulations with a maximum water temperature of 60 °C. A unique aspect of their work is that they used CFD in a more advanced way than in other studies to predict local boiling within the pool water, reflecting the strength of the CFD approach. Another use of CFD is to study flow characteristics within fuel assemblies. For example, a study conducted by Chen et al. [13] investigated flow and heat transfer within a rod bundle using a three-dimensional model.

Yanagi et al. [14] produced a CFD model for a cooling pond and compared the predicted water temperature with those for the cooling pond at Fukushima Daiichi Nuclear Power Station under loss of cooling conditions. The water surface was modelled using a previously derived heat transfer correlation by the same authors [15]. The CFD model produced by Yanagi et al. [14] was further used to form a baseline for an analytical model "One-Region model" also generated by Yanagi et al. [16, 17]. This One-Region treats the water as on node with a single temperature value without taking into considerations its distribution. After that, they have examined the effect of the distribution of the heat load on the variation of water temperature and it was confirmed that the One-Region model applicable to predict the water temperature in the cooling pond during the loss of cooling scenario.

On the other hand, most of the studies adopting the system codes were concerned about investigating accident scenarios and their consequences. Carlos et al. [18] used the TRACE best estimate code to analyse the safety of the Maine Yankee spent fuel pool. Ognerubov et al. [19] investigated scenarios of the loss of water in a spent fuel pool in the Ignalina NPP using various system codes to identify potentially unrealistic parameters while performing the calculations. Groudev et al. [20] used RELAP5 to study the thermal-hydraulic behaviour of spent fuel for a dry out scenario while transferring fuel from the Kozloduy NPP reactor vessel to the cooling pool. Additional studies dealing with fuel ponds can be found elsewhere [5, 21, 22].

Some investigations concern accident mitigation options using thermal-hydraulic codes. Chen et al. [6] used the GOTHIC code to model a spent fuel pool owned by the Taiwan Power Company to analyse its response to spray mitigation under loss-of-coolant scenarios. Wu et al. [23] conducted an analysis of the loss of cooling accident scenarios for a spent fuel pool at the CPR1000 NPP using the MAAP5 code. In the same study, the authors discussed mitigation measures to recover the pool cooling system using make-up water.

The literature cited above shows that the CFD approach is more convenient when it comes to improving the design of cooling ponds, as it offers an in-depth understanding of heat and mass transfer and fluid mixing. On the other hand, thermal-hydraulic system codes such as TRACE are more suitable for analysing safety issues with such ponds and when the system under consideration can be approximated to one-dimensional flow.

In general, most studies focus on investigations of severe accident scenarios and the analysis of their consequences. However, relatively few studies have reported on improving pond design as well as accident mitigation options. Conversely, very limited number of studies have investigated the thermal performance of spent fuel cooling ponds during normal operating conditions, which may represent the first line of defence in accident prevention.

It is worth noting that most spent fuel cooling ponds considered in the cited studies are of relatively small size. On the other hand, due to the continuing increase in spent fuel production, some countries are tending to construct centralised cooling ponds to keep up with demand from incoming spent fuel until a more permanent solution is found [24, 25]. To date, centralised, large-scale, ponds have been little discussed in literature, and this may be attributable to the challenges encountered during the modelling and analysis of such systems.

In this paper, we explore the suitability of adopting the well-mixed approach in developing a Z-D model for a large-scale cooling pond. The well-mixed approach is widely used in ventilation applications to predict the concentration of specific gases or vapours in a room [26]. This model treats the room as a large box, which is perfectly mixed so that the concentration of gas or vapour is uniform.

The proposed Z-Dmodel is able to provide a quick answer for "what-if" scenarios, which is necessary at the decision-making stage to aid organisations in more efficient operation of their cooling ponds. Also, the Z-D model will allow, in future work, the thermal performance of the large-scale cooling ponds to be analysed. Also, the outcomes from the proposed model can be coupled with the numerical approach to provide some boundary conditions in the CFD analysis for both macro and micro level model of the pond. For example, the coupling can be achieved via specifying the boundary condition at the free water surface in the CFD model instead of modelling the humid air zone, which involved multiphase models.

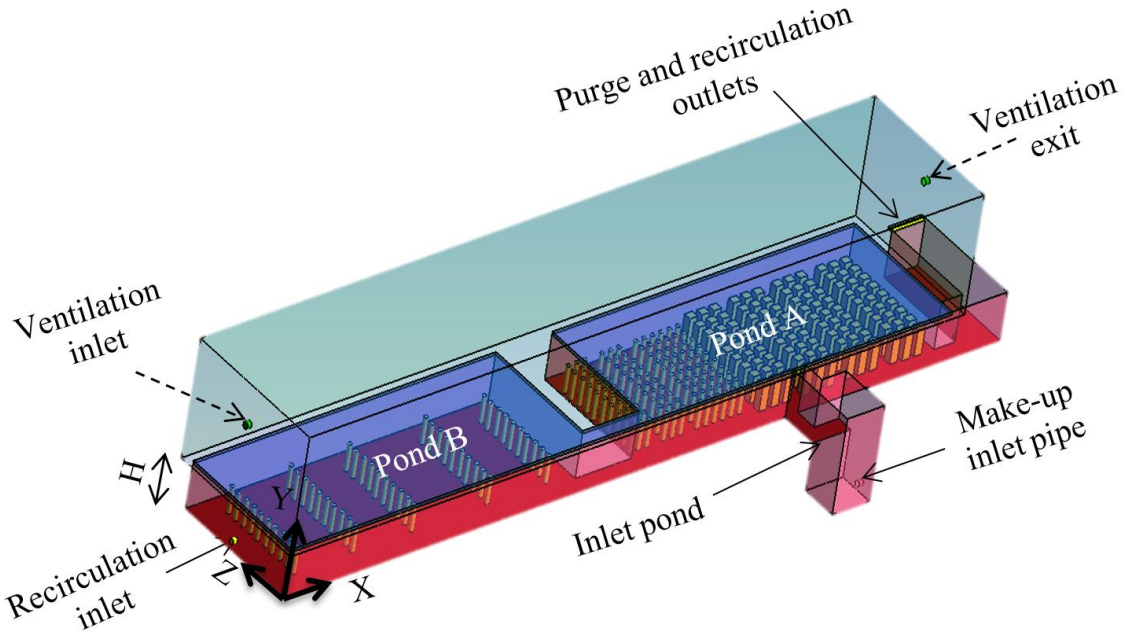

Figure 1. Schematic diagram of the large-scale fuel pond.

2 Large-Scale Cooling Pond under investigation

Figure 1 shows a schematic diagram of the large-scale cooling ponds in a three-dimensional view. The pond are characterised by large dimensions of 160m x 25m x 8m and the water surface area is about 3500 m^2. The whole installation consists of three different ponds. The entire facility includes three different ponds. Pond A and Pond B store the heating sources while the inlet pond supplies make-up. Heat removal takes place via three mechanisms: ventilation, make-up water and water recirculation as illustrated in Figure 2. When the heat is released from the heat sources, the water temperature starts to increase as does the heat transfer from the water surface to the ambient air. The heat transfer from the water surface takes place via three heat transfer modes: evaporation, convection, and radiation. The ventilation system is used to replace the warm air within the building with relatively cooler air. The major heat loss from the water surface is due to the evaporative component; however, this is associated with the loss of pond water, which may lead to a significant drop in the water level in the long term. For this reason, make-up water can be supplied to the pond to prevent the potential risk of uncovering the heat sources. Furthermore, make-up water can be used for purging the pond water as it has been demineralised before reaching the pond. The temperature of the make-up water is mostly determined by the outside temperature.

Recirculation can be used on occasions when cooling by ventilation and make-up water is not sufficient to control the pond temperature. Cooling via recirculation is achieved by feeding some of the pond water through a cooling tower which then re-enters the pond a few degrees cooler. However, cooling is not the only function of recirculation. It also helps to reduce unfavourable thermal stress in the pond's concrete walls which may otherwise lead to cracks and the leakage of contaminated water. This is achieved by maintaining the water temperature as uniformly distributed as possible, preventing excessive cracking in the pond walls.

Also, due to the long storage time of the heat load under water, a caustic dosing is injected to protect the fuel cladding from any potential corrosion as well as to assist with the removal of colour and turbidity present in the cooling water. In addition, the operational experience showed that such chemical could help to reduce cracks in the concrete walls. In such situation, recirculation of the pond water is required to improve the dispersion of the caustic dosing by recirculating the pond water at various locations across the pond.

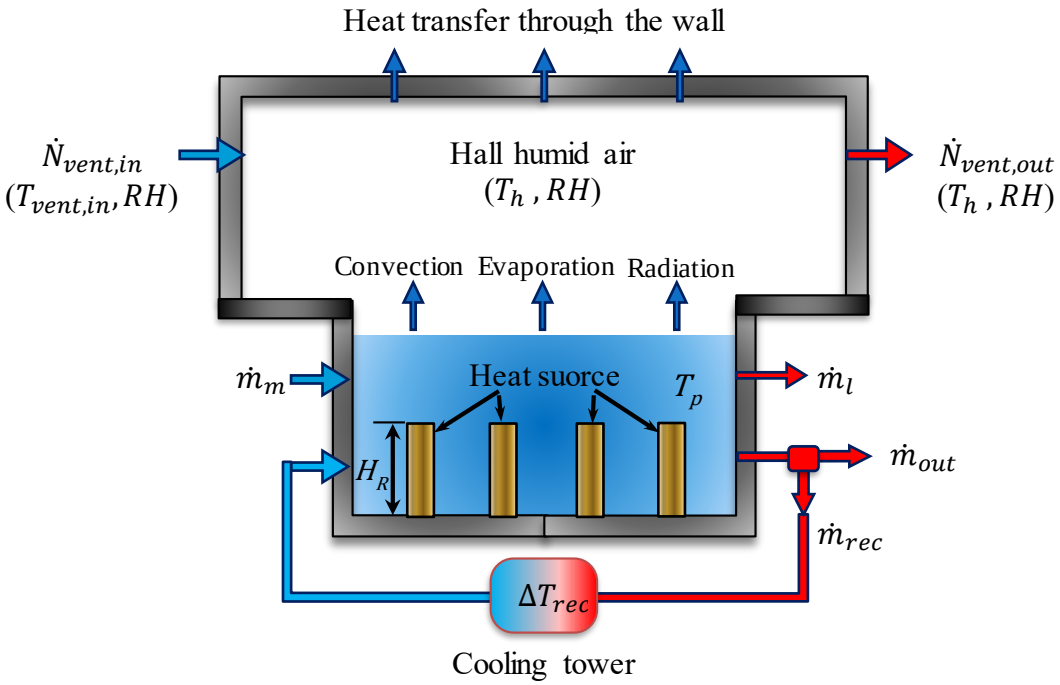

Figure 2. Description of the processes taking place within the pond installation.

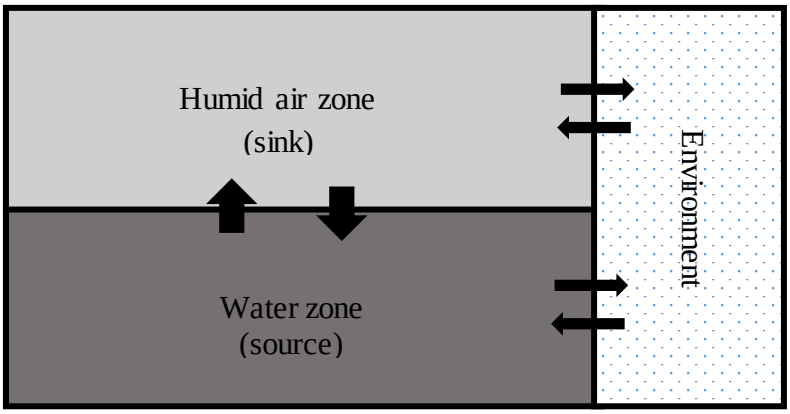

Figure 3. Zones used in the Z-D model.

3 Z-D Model

While developing the Z-D model for the cooling ponds, the whole pond installation is divided into two nodes: the humid air zone and water zone as shown in Figure 3. These zones can be described as a source and a sink, where the water zone acts as the source of water vapour and

heat energy and humid air zone acts as the sink. Energy and mass transfer with the environment, the third zone, is also integral part of the model

The well-mixed approach is adopted in both zones. Since the heat sources are located at the bottom of the pond, the water temperature for the bulk of the pond can be assumed to be uniformly distributed due to buoyancy-induced convection. Similarly, the temperature of the humid air zone can be treated a single value due to the large volume and the flow process of evaporation. Experimental data from the site also support the above assumption.

The proposed Z-D model is based on solving conservation of mass and energy equations for the water body and humid air zone above the water surface. The model treats each zone as a single control volume and takes into account heat and mass transfer as well as interaction at the air-water interface. The environment provides some boundary conditions such as temperature and relative humidity to solve the ODEs involved water and humid air zones.

The forward time marching approach is adopted to solve a system of differential equations of mass and energy using Euler's forward method as a discretization scheme [27]. This is an explicit method where the solution of the current time step depends on information from the previous step. The general form of Euler's method is shown in Eq. (1). The advantage of this approach is that it does not require significant computing time or power and allows the calculations to be performed using Microsoft Excel spreadsheet

$$x^{n+1} = x^n + f(t^n, x^n)\Delta t \quad (1)$$

A diagrammatic representation of the Z-D model is illustrated in Figure 4. In the beginning, initial values are given to start the solution. The physical properties of air and water are evaluated at each time step. After that, the mass fluxes across the pond structure, evaporation and condensation rates, are estimated along with the ventilation discharge rate. At this point, two mass balance equations are solved in order to calculate the amounts of air and water, which are needed to solve the energy equation in each zone. Finally, air and water temperatures are obtained for this time step. The new temperature will be used to recalculate the physical properties of air and water for the next time step. This is an iterative process that will continue until the steady state is reached.

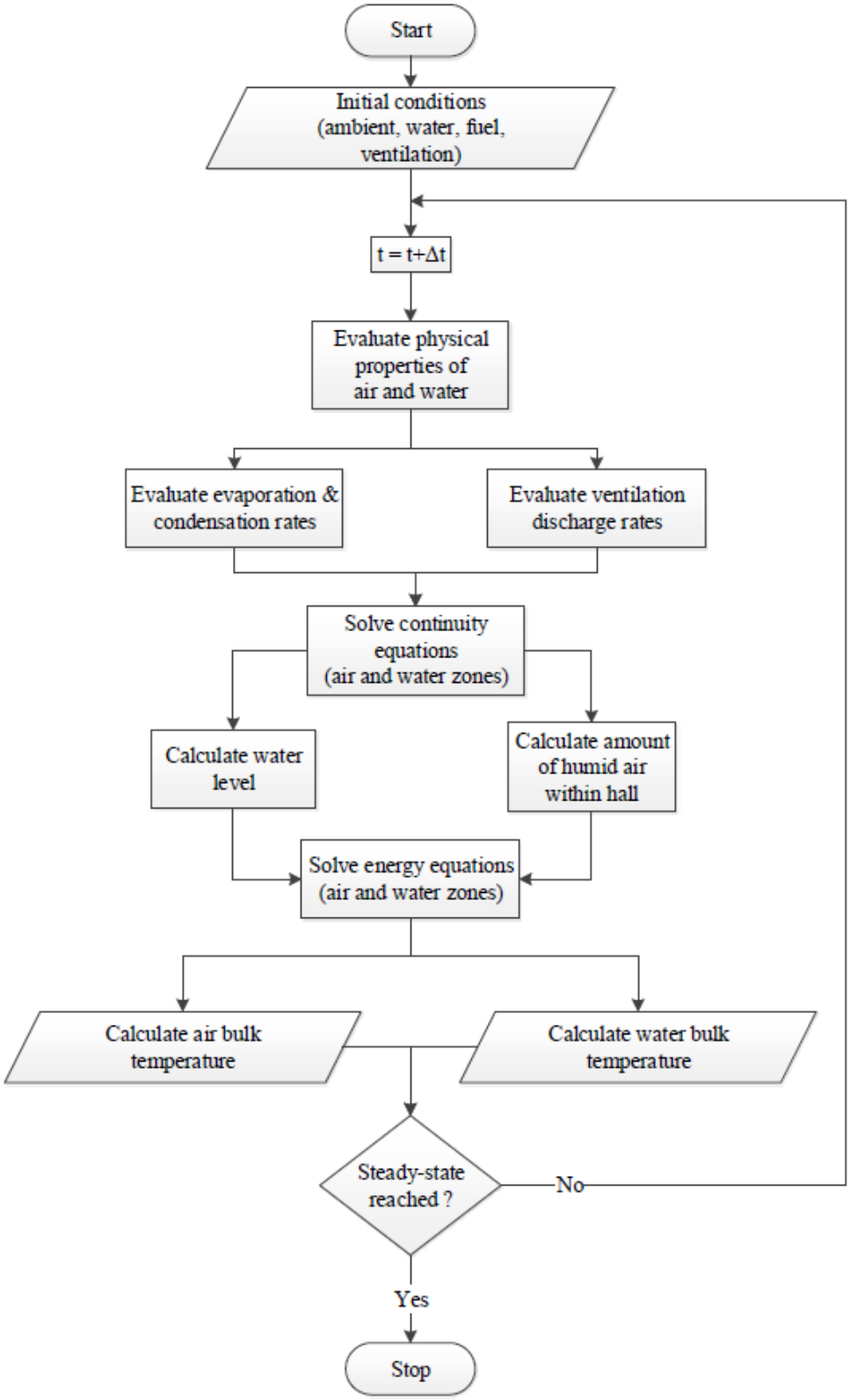

213

214 Figure 4. Flowchart representation of the Z-D model.

215

3.1 Mass Balance of the Water Zone

The water in the pond is evaluated at each time step, considering any change due to the supply of make-up water ($\dot{m}_m$) and loss of water due to evaporation ($\dot{m}_{ev}$), leakage ($\dot{m}_l$), and water outflow ($\dot{m}_{out}$). Therefore, the mass balance equation for pond water can be written as follows:

$$m_p^{n+1} = m_p^n + (\dot{m}_m - \dot{m}_{out} - \dot{m}_{ev} - \dot{m}_l)^n \, \Delta t \tag{2}$$

where m_p is the total mass of water within the ponds, Δt is the time step size, and n is the number of iterations.

The following equation describes how the water outflow from the pond is controlled. When the water loss due to evaporation and leakage is greater than the supplied make-up water, no water discharge will be permitted. Similarly, in situations when the height of the water level (H) is lower than its designed value (H_D), no water outflow is allowed until the water level reaches this value. The following relationship explains how the outflow of water can be mathematically expressed:

$$\dot{m}_{out} = \begin{cases} 0 & if \quad (\dot{m}_{ev} + \dot{m}_l) \geq \dot{m}_m \\ \dot{m}_m - \dot{m}_{ev} - \dot{m}_l & if \quad (\dot{m}_{ev} + \dot{m}_l) < \dot{m}_m \\ 0 & if \quad H \leq H_D \\ \left[\dfrac{\rho_w \, A_p (H - H_D)}{\Delta t}\right] + (\dot{m}_m - \dot{m}_{ev} - \dot{m}_l) & if \quad H > H_D \end{cases} \tag{3}$$

where ρ_w is the water density and A_p is the water surface area of the pond. The evaporation rate before the pond water starts to boil can be estimated using Stefan's law [28]. The following equations show how the evaporation rate can be estimated before boiling and in the case of boiling.

$$\dot{m}_{ev} = \begin{cases} h_{ev}\, log\left(\dfrac{P_t - P_{v,s}}{P_t - P_{v,\infty}}\right) A_p & if\ T_p < T_{sat} \\ \dot{Q}_d / h_{fg} & if\ T_p \geq T_{sat} \end{cases} \quad (4)$$

where, $P_{v,s}$ is the saturated vapour pressure at surface temperature, and $P_{v,\infty}$ is the vapour pressure at the hall temperature, P_t is the total pressure of humid air inside the hall, h_{fg} is the latent heat of vaporization for water, $\dot{Q}_d$ is the released heat from the heating elements, T_p is the pond water temperature, T_{sat} is water saturation temperature and h_{ev} is the evaporative mass transfer coefficient which can be calculated using the analogy between heat and mass transfer using Sherwood–Rayleigh power law, $Sh - Ra$, as shown below [28]:

$$Sh = \begin{cases} 0.54\ {Ra_{ev}}^{1/4} & if\ 10^4 \leq Ra_{ev} \leq 10^7 \\ 0.15\ {Ra_{ev}}^{1/3} & if\ 10^7 \leq Ra_{ev} \leq 10^{11} \end{cases} \quad (5)$$

where Ra_{ev} is the Rayleigh number for mass transfer by evaporation. The definition of Ra_{ev} can be expressed as shown below:

$$Ra_{ev} = Gr.Sc = \left(\frac{g\Delta\rho L^3}{\rho_{av}\nu^2}\right).Sc \quad (6)$$

here Gr is the Grashof number and L is the characteristic length, which is considered to be the area of the water surface over its perimeter.

3.2 Pond Water Elevation

The pond water level is calculated by knowing the water volume and the surface area of the pond water. When the water level drops to a value less than the rack height (H_R) shown in Figure 2, the surface area of the water will be limited to the surface area of water between the

rack assemblies (A_R). The water level at every time step is updated according to the mass of water available in the pond, as shown in the following equation:

$$H = \begin{cases} \left[\left(\frac{m_p}{\rho_w} - A_R H_R\right)/A_p\right] + H_R & if \quad H \geq H_R \\ \left(\frac{m_p}{\rho_w}\right)/A_R & if \quad H < H_R \end{cases} \tag{7}$$

3.3 Mass Balance of the Humid Air Zone

Humid air is considered as a mixture of dry air and water vapour. Both dry air and water vapour at low partial pressure can be treated as a perfect gas. When dealing with humid air, it is more convenient that the mass of the moist air to be expressed in mole basis for the dry air and vapour separately.

In order to evaluate the amount of dry air (N_a) and vapour (N_v) inside the pond hall, the mass balance equation across the hall is applied as shown in Equations (8) and (9). This mass balance takes into account the ventilation inlet ($\dot{N}_{vent,in}$) and discharge ($\dot{N}_{vent,out}$) flow rates as well as evaporation and condensation ($\dot{m}_{con}$) rates.

$$N_a^{n+1} = N_a^n + \left(y^a_{vent,in}\, \dot{N}_{vent,in} - y_h^a\, \dot{N}_{vent,out}\right)^n \Delta t \tag{8}$$

$$N_v^{n+1} = N_v^n + \left(\dot{N}_{vent,in} - y_h^v\, \dot{N}_{vent,out} + \frac{\dot{m}_{ev}}{M_v} - \frac{\dot{m}_{con}}{M_v}\right)^n \Delta t \tag{9}$$

where $y^a_{vent,in}$ is the molar fractions of dry air of the incoming ventilation air and y_h^a and y_h^v are the molar fractions of dry air and water vapour respectively, which can be found from:

$$y_h^a = \frac{N_a}{N_h} \tag{10}$$

$$y_h^v = \frac{N_v}{N_h} \tag{11}$$

$$N_h = N_a + N_v \tag{12}$$

Here N_h is the total molar mass of the humid air inside the pond hall. The flow rate of the ventilation inlet is an initial input condition, where the differential pressures drive the ventilation discharge and can be computed from:

$$\dot{N}_{vent,out} = \rho_\infty M_v A_{duct} \sqrt{\frac{2(P_t - P_{atm})}{\rho_\infty}} \tag{13}$$

where ρ_∞ is the density of the humid air inside the pond hall, M_v is the molecular weight of water vapour, A_{duct} is the cross-sectional area of the ventilation discharge duct, P_{atm} is the outside atmospheric pressure P_t is the total pressure of humid air inside the pond hall and can be evaluated as follow:

$$P_t = \left(\frac{T_h R_o}{V_h}\right) N_h \tag{14}$$

The estimation of the condensation rate is similar to the calculation of the evaporation rate:

$$\dot{m}_{con} = h_{con}\left(\rho_{v,\infty} - \rho_{v,wall}\right) A_h \tag{15}$$

where, $\rho_{v,wall}$ is the saturated vapour density at wall temperature, A_h is surface area of the inner walls of the pond hall and h_{con} is the condensation mass transfer coefficient which can be calculated from:

$$Sh = 0.10\ Ra^{1/3} \tag{16}$$

To examine the coefficient 0.10 in Eq. (16), we have run several calculations considering different values for this coefficient ranging from 0.05 to 0.2. It was found that the maximum effect of this coefficient on the final result for the water temperature is relatively low, less than 1.5%.

3.4 Energy Balance of the Water Zone

The energy contained in the water body is integrated over time taking into account the heat realised from the heat sources, the heat flux from the water surface and the energy associated with the water inlets and outlets:

$$T_p^{n+1} = T_p^n + \left(\dot{Q}_d + \dot{m}_m C_w T_m - \dot{m}_{out} C_w T_p - \dot{m}_{ev} C_w T_p - \dot{m}_{rec} C_w \Delta T_{rec} - \dot{Q}_s\right)^n \frac{\Delta t}{m_p C_w} \tag{17}$$

where C_w is the specific heat of water, T_m is the temperature of the make-up water, $\dot{m}_{rec}$ is the recirculation flow rate, ΔT_{rec} is the temperature drop in the cooling tower which is controlled by the wet bulb temperature of the outdoor air (T_{wb}) and the cooling tower efficiency and can be expressed as:

$$\zeta = \frac{\Delta T_{rec}}{T_p - T_{wb}} \tag{18}$$

and $\dot{Q}_s$ is the total heat transfer at the air-water interface which can be estimated as shown below:

$$\dot{Q}_s = \dot{Q}_{ev} + \dot{Q}_r + \dot{Q}_c \tag{19}$$

317

318 where $\dot{Q}_{ev}$ is the evaporative heat transfer, $\dot{Q}_r$ is the radiative heat transfer, and $\dot{Q}_c$ is the
319 convective heat transfer. These three heat transfer modes can be evaluated from the following
320 expressions:

321

$$\dot{Q}_{ev} = \dot{m}_{ev} h_{fg} \tag{20}$$

322

$$\dot{Q}_r = A_p \varepsilon \, \sigma ({T_p}^4 - T_{wall}^4) \tag{21}$$

323

$$\dot{Q}_c = A_p h_c (T_p - T_h) \tag{22}$$

324

325 Here ε is emissivity, σ is the Stefan Boltzmann constant, T_{wall} is the wall inner surface
326 temperature of the hall, h_c is the convection heat transfer coefficient at the water surface which
327 may be evaluated by using the Nusselt– Rayleigh power law, $Nu - Ra$, as shown below:

328

$$Nu = \begin{cases} 0.54\, Ra^{1/4} & if\ \ 10^4 \leq\ Ra\ \leq 10^7 \\ 0.15\, Ra^{1/3} & if\ \ 10^7 \leq\ Ra\ \leq 10^{11} \end{cases} \tag{23}$$

329

330 ***3.5 Energy Balance of the Humid Air Zone***

331 The heat loss from the water surface is gained by the ventilated air, which results in an increase
332 in air temperature. To calculate the air temperature inside the pond hall, the energy balance is
333 performed across the hall as shown below:

334

$$T_h^{n+1} = T_h^n + \left[\dot{m}_{ev} h_v(T_p) + \dot{Q}_c + \dot{Q}_r - \dot{Q}_{wall} - \dot{m}_{con} h_{fg} + \dot{Q}_{vent,in} - \dot{Q}_{vent,out}\right]^n \frac{\Delta t}{\left[N_a M_a C_{p,a} + N_v M_v C_{p,v}\right]} \tag{24}$$

where $h_v(T)$ is the specific enthalpy of water vapour at a given temperature and can be calculated using the shown below [29]. However, this relationship is valid only for low values of pressure.

$$h_v(T) = 2500 + 1.82\,(T - 273) \tag{25}$$

In order to obtain the heat energy associated with the incoming ventilated humid air ($\dot{Q}_{vent,in}$) and the discharged humid air by ventilation ($\dot{Q}_{vent,out}$), the following relationships are used:

$$\dot{Q}_{vent,in} = y^a_{vent,in}\,\dot{N}_{vent,in} C_{p,a} T_{vent,in} + y^v_{vent,in} \dot{N}_{vent,in} h_v\left(T_{vent,in}\right) \tag{26}$$

$$\dot{Q}_{vent,out} = y^a_h\,\dot{N}_{vent,out} C_{p,a} T_h + y^v_h\,\dot{N}_{vent,out} h_v(T_h) \tag{27}$$

Here, $y^a_{vent,in}$ and $y^v_{vent,in}$ are the molar fractions of the ventilation inlet dry air and vapour respectively, $C_{p,a}$ is the specific heat of the dry air, and $T_{vent,in}$ is the ventilation inlet temperature which is assumed to be the same as the outside temperature. The heat transfer through the walls of the pond hall ($\dot{Q}_{wall}$) is computed according to:

$$\dot{Q}_{wall} = h_{in}(T_h - T_{wall})\,A_h \tag{28}$$

In order to determine T_{wall}, an energy balance is performed across the walls of the pond hall where the wall thickness (x) is divided to uniform increments of dx. The energy equations for the interior and surface layers can be written as follow:

$$T_i^{n+1} = T_i^n + \frac{k}{dx\ C_{wall}\rho_{wall}}\left(\frac{T_{i-1} - T_i}{dx} - \frac{T_i - T_{i+1}}{dx}\right)^n \Delta t \quad (29)$$

356

$$T_i^{n+1} = T_i^n + \frac{k}{dx\ C_{wall}\rho_{wall}}\left(\frac{T_{wall} - T_i}{dx/2} - \frac{T_i - T_{i+1}}{dx}\right)^n \Delta t \quad (30)$$

357

358 where i is the index of the wall layers, C_{wall} is the specific heat of the walls material, ρ_{wall} is
359 the density of the walls material, and k is the thermal conductivity of the walls material. The
360 inner and outer surface temperatures can be calculated considering the heat balance across this
361 surface as shown below, respectively:

362

$$\dot{Q}_r + (T_h - T_{wall})A_h h_{in} = \frac{T_{wall} - T_i}{dx/2} A_h k \quad (31)$$

363

$$(T_{out} - T_{env})A_h h_{0ut} = \frac{T_i - T_{out}}{dx/2} A_h k \quad (32)$$

364

365 where T_{env} is the outside environment temperature h_{in} is the convective heat transfer
366 coefficient for the inner surface of the pond hall and h_{0ut} is the outer surface heat transfer
367 coefficient and was considered to be constant (4 W/m^2 K). Finally, under the normal
368 operational conditions, the solution is considered to be converged when the relative difference
369 between the current iteration and the previous iteration is less than 0.01%. The convergence
370 criterion is expressed as shown below:

371

$$\text{Convergence criterion} = \frac{|T_p^{n+1} - T_p^n|}{T_p^n} \times 100 \quad (33)$$

372

373 However, this convergence criterion cannot be applied when the pond is suffering from loss of
374 cooling. In this case, the temperature of the pond water will continue to increase until the

saturation is reached. During this time, the water level may drop until the pond dries out unless sufficient make-up water is provided to compensate for the evaporated water.

The heat loss from the pond water to the concrete wall is not considered in this study as it makes only a tiny contribution to the total heat loss from the pond's structure. This is because the ponds are surrounded by a very thick concrete layer at the sides and floor.

As mentioned before, the calculations were performed using the explicit Euler's method, which is known to be conditionally stable, hence, a stability analysis is required [30]. Investigation of the numerical behaviour of the model shows that the stability of the model is more dominated by the stability of the differential equations rather than the used method. The highest instability was observed in the mass balance equation for the humid air zone. This is due to the pressure fluctuation, which is mostly controlled by the ventilation discharge. Therefore, a stability analysis is conducted on the mass balance equation for the humid air zone. However, to perform such analysis, the nonlinear equations have to be linearized. The linearization of the ODE for the mass balance of the humid air zone was achieved using Taylor series. Then, a systematic stability analysis was accomplished as follows:

- Construct the finite difference equation (FDE) for the model ODE, $\acute{y} + \phi y = 0$
- Determine the amplification factor, G, of the FDE.
- Determine the conditions to ensure that $|G| < 1$.

By applying the above-mentioned practice, an estimation of the limit of the stable time step can be expressed as:

$$\Delta t < \frac{2}{\theta} \tag{34}$$

where θ is equivalent to:

$$\theta = \frac{A_{duct} R_o T_h}{2V_h} \sqrt{\frac{2\rho_\infty}{\left(\frac{T_h R_o}{V_h}\right) N_h^n - P_{atm}}} \tag{35}$$

Note that θ changes as N_h^n changes. Thus, the stable step size changes as the solution advances. However, keeping the time step within the criterion shown in Eq. (34) not only ensures stability, but it also ensures that the results are not very sensitive to the time step. According to this criterion, the used time step in all the cases presented in this study is 5 sec.

4 Z-D Model Validation

The Z-D thermal model of the cooling pond is validated against available data for two different cooling ponds as shown below:

1. Maine Yankee spent fuel pool, Wiscasset, USA [18]
2. The large-scale cooling pond

4.1 Validation with Maine Yankee Pool Data

The Maine Yankee spent fuel pool is a relatively small cooling pond located at the reactor site, with dimensions of 12.6 m long, 11.3 m wide and 11.1 m deep. Carlos et al. [18] used TRACE best estimate code to analyse the response of the cooling pond in different scenarios. During their calculations, no heat loss was considered at the free water surface except when the water has reached its saturation temperature (100 ^{o}C) with the initiation of boiling. However, this assumption does not have a significant effect on the results, as the proportion of heat loss from the water surface before boiling is not significant compared to the heat loss by the supplied water. This is owing to the small surface area at the air-water interface.

The Z-D model is used to perform calculations on the Maine Yankee spent fuel pool, Wiscasset, USA [18] and the results obtained are compared against the published data for this pool. These calculations are developed for three cases: (a) steady-state, (b) licensing, and (c) accident scenarios.

In the paper reported by Carlos et al. [18], the temperature data were available for the steady-state case in the form of actual temperature measurements collected from the Maine Yankee spent fuel pool. For the licensing case, the temperature data were calculated by GFLOW software [31], while the TRACE best estimate code was used for the pool temperature under the accident scenarios.

(a) - (b) Steady-state and Licensing Cases

The input parameters used in the calculations of the steady-state and licensing cases are summarised in Table 1. In the same table, the outcomes from the validation exercise our Z-D model are presented. The heat load in the licensing case corresponds to the maximum expected heat generation from the fuel elements.

The results predicted by the Z-D model are in good agreement with the available data for the Maine Yankee spent fuel pool as can be seen in Table 1. However, the Z-D model underestimates the pond water temperature by 3 % and 2.6 % for steady-state and licensing cases respectively. When all of the heat transfer modes from the water surface are deactivated in the Z-D model calculations, except for boiling, the underestimation errors of the water temperature decreased to 1.9 % and 0.9 % for the steady-state and licensing cases respectively. This implies that the heat loss from the water surface before boiling is relatively less significant, as mentioned before.

Table 1. Input data and comparison between values predicted by the Z-D model and data for the Maine Yankee pool [18].

Parameters / Case		Steady State Case	Licensing Case
Heat load (MW)		3.3	6.4
Make-up water flow rate (kg/s)		98	97.6
Make-up water temperature (^{o}C)		26.1	51.7
Water bulk temperature (^{o}C)	Maine Yankee pool [18]	**36.7** (measured)	**68** (GFLOW)
	Present Z-D model	35.6	66.2
	errors	- 3 %	- 2.6 %

(c) Accident Case

The outcomes from the licensing case were used as the input data for the accident scenario except for the initial water level which is considered to have a value of 4.56 m as measured from the bottom of the pond. In the TRACE simulation for the accident case, it was assumed that the pumps which supply the pond with the cooling and make-up water, have stopped functioning and the only heat loss mechanism available is the heat loss to the surroundings by

means of boiling. Therefore, in the Z-D model calculations, the heat transfer modes from the water surface were deactivated and the only heat transfer permitted is due to boiling.

Figures 5 and 6 show comparisons between the results predicted by the Z-D model and the TRACE data for the accident scenario in terms of water temperature and drop of pond water level respectively. In Figure 5, for up to one hour the same linear trend is observed, but a clear shift of 1.8 ^{o}C is recorded, the reason for which is not obvious from the original paper [18]. Figure 6 shows a sudden drop in water level over a very short time (something similar to purging), but the reason for such behaviour was also not explained. These behaviours may be due to assumptions made which are unknown to us. In general, good agreement can be observed between the Z-D model and the TRACE best estimate code.

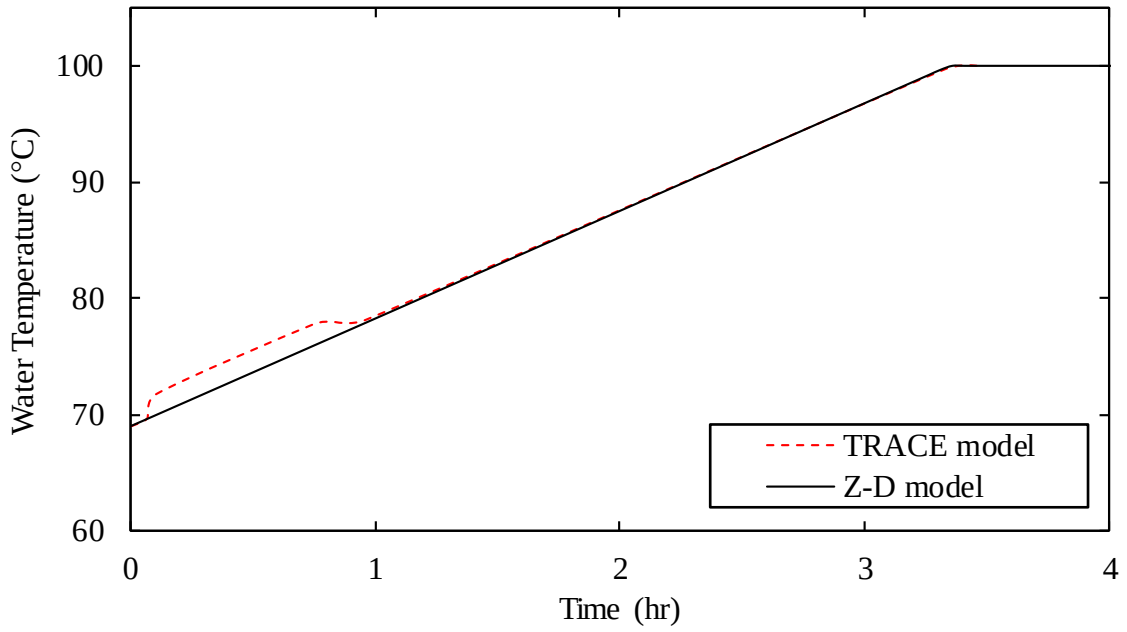

Figure 5. Comparison of water temperature for the accident case that obtained by the proposed Z-D model and Maine Yankee pool [18].

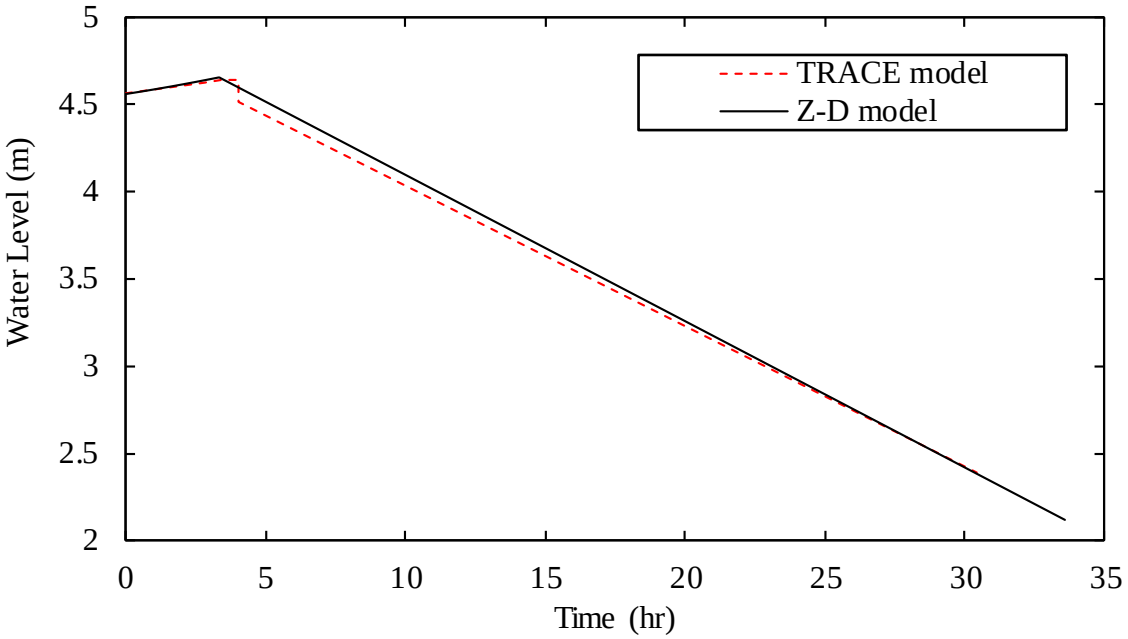

Figure 6. Comparison of water level for the accident case that obtained by the proposed Z-D model and Maine Yankee pool [18].

4.2 Validation with Large-Scale Cooling Pond Data

The validation exercise is further extended to consider a large-scale cooling pond to examine the effect of pond size on the Z-D model's prediction. The total heat realised from the heat sources is about 340 kW.

The validation is performed for three different operational configurations and the input parameters used during these calculations are summarised in

Table 2. Comparisons between the measured data and the results predicted by the Z-D model are presented in tabular form as shown in Table 3. It can be seen from the comparisons that the Z-D model has predicted the water temperature as well as the hall air temperature within a good level of accuracy. However, the Z-D model has slightly overestimated the water temperature. The maximum observed error in the predictions of water temperature is 3.56 %, where the maximum recorded error in the hall air temperature is - 4.55 %.

Table 2. Input parameters used in validation with the large-scale cooling pond data.

Parameters	Case 1	Case 2	Case 3
Initial water level (m)	8	8	8
Water surface area (m^2)	3,500	3,500	3,500
Water zone volume (m^3)	21,900	21,900	21,900
Humid air zone volume (m^3)	129,600	129,600	129,600
Heat transfer area of humid air zone (m^2)	15,120	15,120	15,120
Heat load (kW)	340	340	340
Outside environment temperature (^oC)	11	14	19
Recirculation flow rate (kg/s)	4.57	4.63	4.05
Temperature drop in cooling tower (^oC)	0	0	3
Make-up rate (kg/s)	3.47	3.62	3.84
Make-up temperature (^oC)	10	14	20
Ventilation inlet rate (m^3/s)	12	12	12

Table 3. Comparison between measured and predicted results for the large-scale cooling ponds data.

	Water Temperature (^oC)			Hall Air Temperature (^oC)		
	Measured	Predicted	Error (%)	Measured	Predicted	Error (%)
Case 1	20.6	21.3	3.39 %	18.2	17.5	- 3.85 %
Case 2	23.2	23.9	3.01 %	19.8	18.9	- 4.55 %
Case 3	25.3	26.2	3.56 %	21.7	21.1	-2.76 %

The percentage contribution of each heat removal mode to the total heat loss is shown in Figure 7 for the three validation cases. These contributions are evaluated when the steady state is reached. From the results shown in this figure, it is obvious that the heat loss from the water surface is significant as it represents about 50% of the total heat loss from the ponds. However,

under different configurations, these ratios can vary significantly. For an instant, when the make-up water or recirculation flow rates are high, this will lead to much higher contributions of these heat removal modes over the surface heat loss.

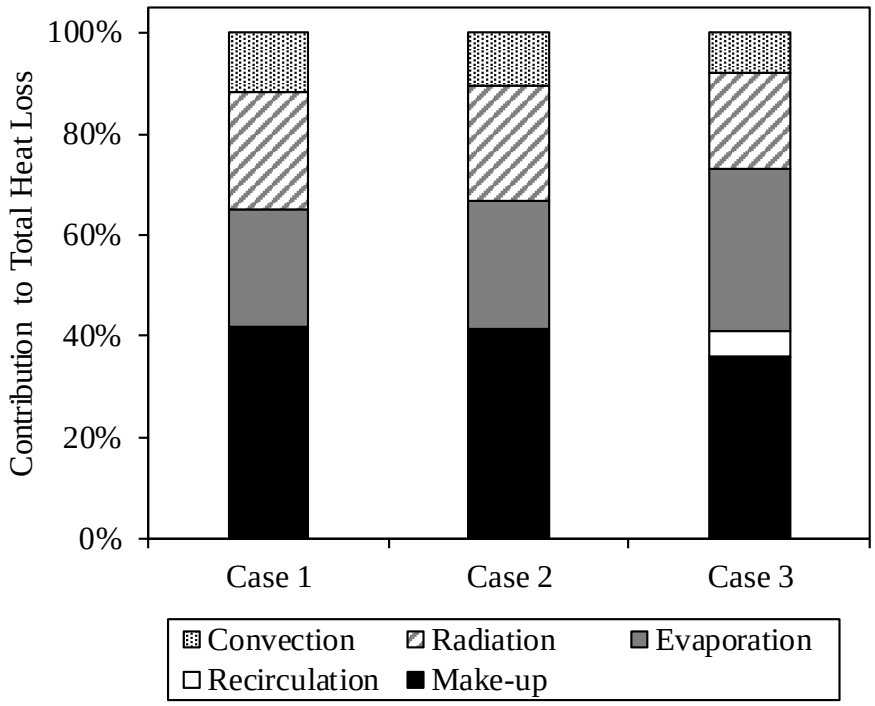

Figure 7. Contribution percentage of different heat removal modes for validation case 1, case 2, and case 3.

5 Analysis of Pond Behaviour

After confirming the reliability of the Z-D model, it was used to study the thermal behaviour of the large-scale cooling pond, and in addition, to assess the suitability of using particular assumptions in certain cases. From the point of view safety and economics, it is essential to analyse the performance of the pond under normal operating conditions as well as accident scenarios.

5.1 Normal Operating Conditions

The calculations in this section are performed considering that the pond is loaded with the maximum possible heat load and all of the cooling systems are in place and under control. The maximum heat load is 11 MW, which corresponds to the maximum expected amount of heat sources to be stored and is assumed to be uniformly distributed throughout the pond. The input parameters used in this calculation are listed in Table 4.

514

515 Table 4. Configurations used in the case of normal operating conditions.

Parameters	
Initial water level (m)	8
Water surface area (m^2)	3500
Water zone volume (m^3)	21900
Humid air zone volume (m^3)	129600
Heat transfer area of humid air zone (m^2)	15120
Heat load (MW)	11
Outside environment temperature (^oC)	14
Recirculation flow rate (kg/s)	115.74
Cooling tower efficiency (%)	60
Make-up rate (kg/s)	13.9
Make-up temperature (^oC)	14
Ventilation inlet rate (m^3/s)	12

516

517 The results for the normal operations case are presented in Figure 8 in terms of water and hall
518 temperatures. As shown in this figure, at the beginning of the calculations the water and air
519 temperatures have the same value of 14 ^oC. As time progresses, both water and air temperatures
520 increase until the steady state is reached at values of 41.5 ^oC for the water and about 31.3 ^oC
521 for the hall air.

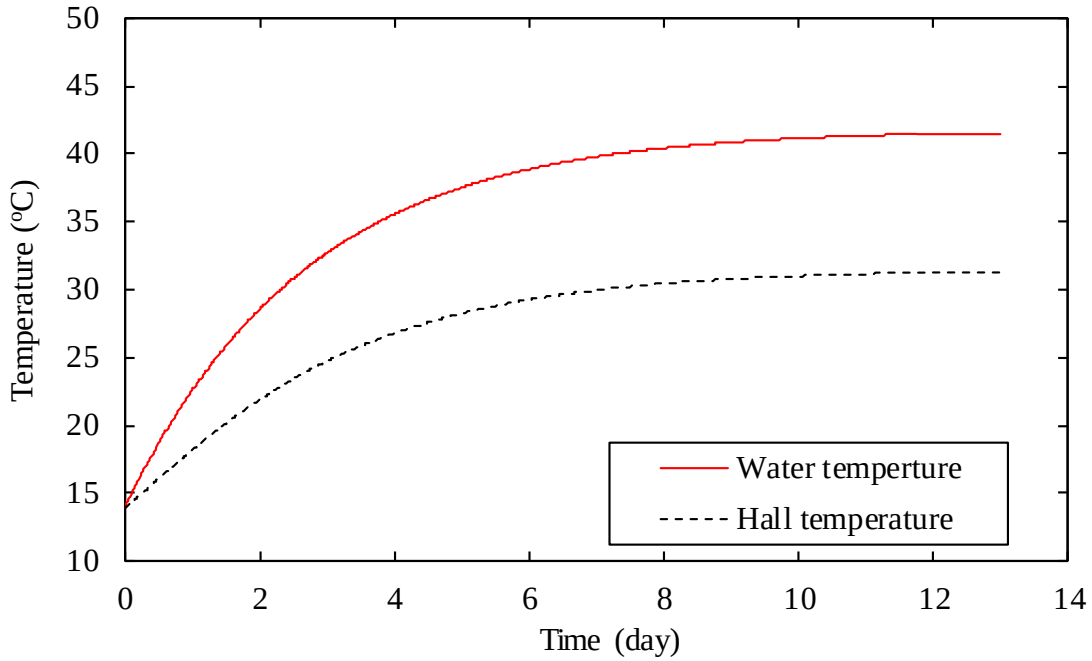

522

523 Figure 8. Water and air temperatures under normal operating conditions for the large-scale
524 cooling pond at a heat load of 11 MW.

525

526 The generated heat is removed via different modes as shown in Figure 9. Furthermore, this
527 figure illustrates the contribution of the heat removal component to the total heat removed from
528 the water body. The generated heat being removed by the recirculation is dominated the cooling
529 process with a percentage of 75 % of the total heat loss. It appears that the heat loss from the
530 water surface represents a relatively small proportion (8%) of the total heat loss, but it cannot
531 be ignored. However, the scenario can be different for lower heat loads as in the cases presented
532 in the validation section for the large-scale cooling ponds as shown in Figure 7.

533

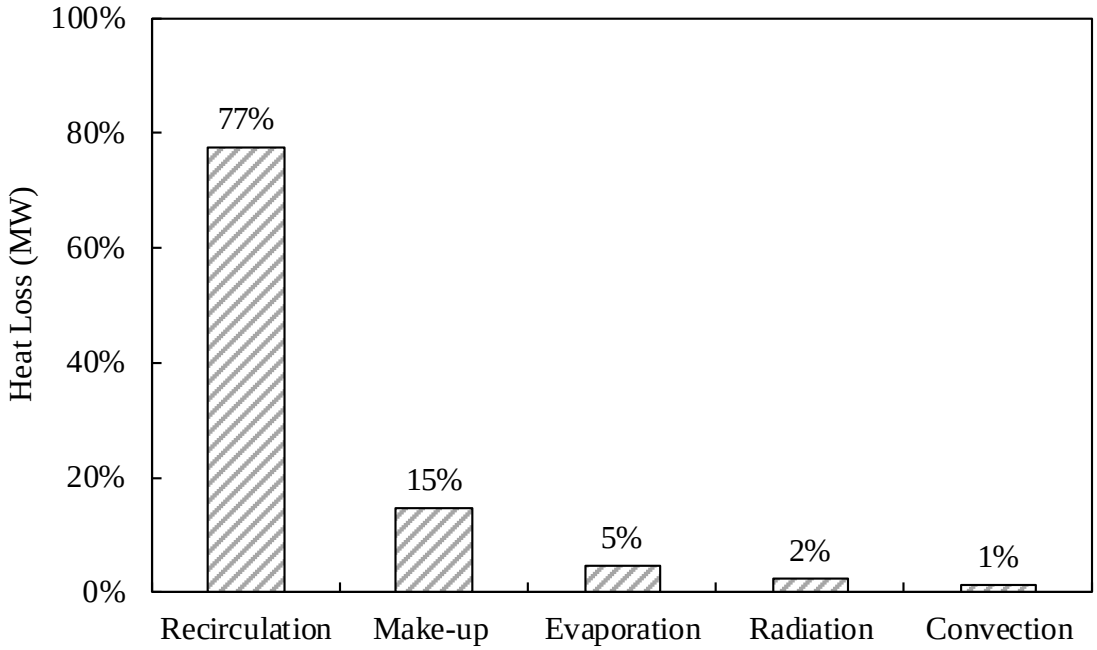

Figure 9. The contribution of different heat removal modes under normal operating conditions for the large-scale cooling pond.

5.2 Loss of Cooling Scenario

In this section, we assume that a power blackout and total loss of the cooling systems occurs with no accident mitigation measures are in place. The calculations are conducted for the large-scale cooling pond taking the outcomes from the previous case of normal operating conditions as initial values. Moreover, the calculations are performed for two different conditions at the water surface. The first condition ignores the heat loss from the water surface except for the boiling heat transfer, which is represented in the graphs by "Heat off". The second condition takes into account all the heat transfer modes at the water surface, which is represented in the graphs by "Heat on".

As can be seen from Figures 10 and 11 that at the "Heat off" condition, the water temperature reaches boiling after 5.6 days. Meanwhile, the water level reaches its highest value due to a decrease in water density and then starts to drop until the fuel assemblies begin to be uncovered at approximately day 37. At this point, make-up water is injected to recover the pond water temperature and level. To achieve this, 2.5 days is required to recover the water level and 18 days for the water temperature to drop to about 50.7 °C.

For the “Heat on” condition, the estimation of the time required for the fuel assembly to start to be uncovered is the same as in the “Heat on” case. On the other hand, water reaches its saturation temperature 2 days earlier than the predicted time in the “Heat on” case. However, these differences, in the presented case, are still within a good level and provide a conservative treatment for the accident scenario. For different conditions, the assumption that the heat loss from the water surface can be neglected may not be appropriate. For example, Figure 12 shows the effect of heat load on the validity of this assumption for different heat loads.

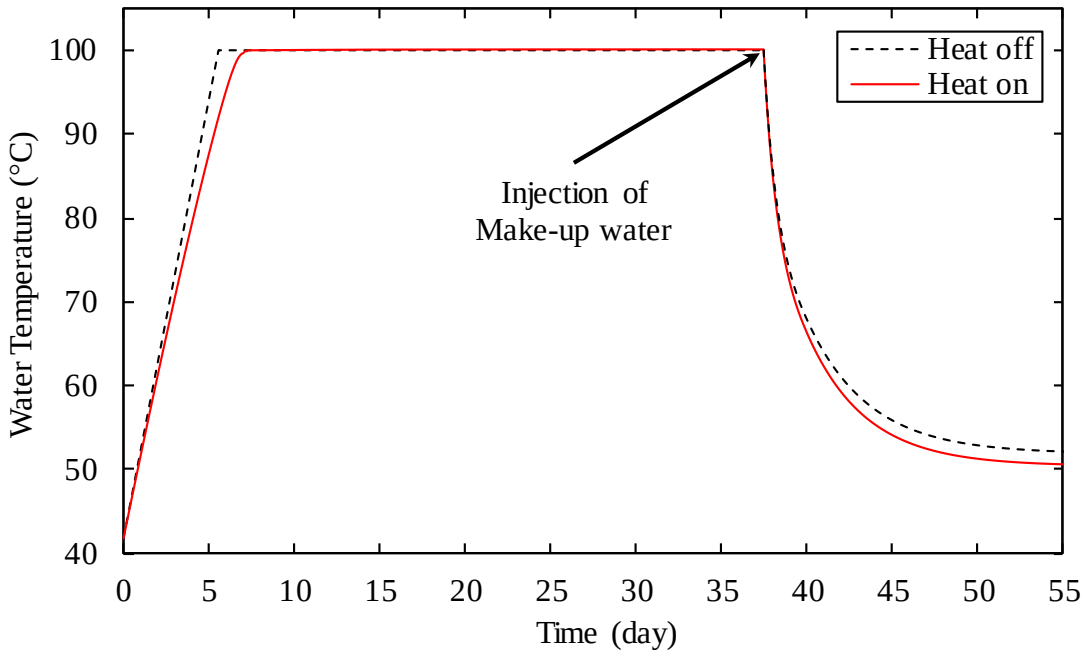

Figure 10. Water temperature during the loss of cooling scenario and after injection of make-up water for the large-scale cooling pond.

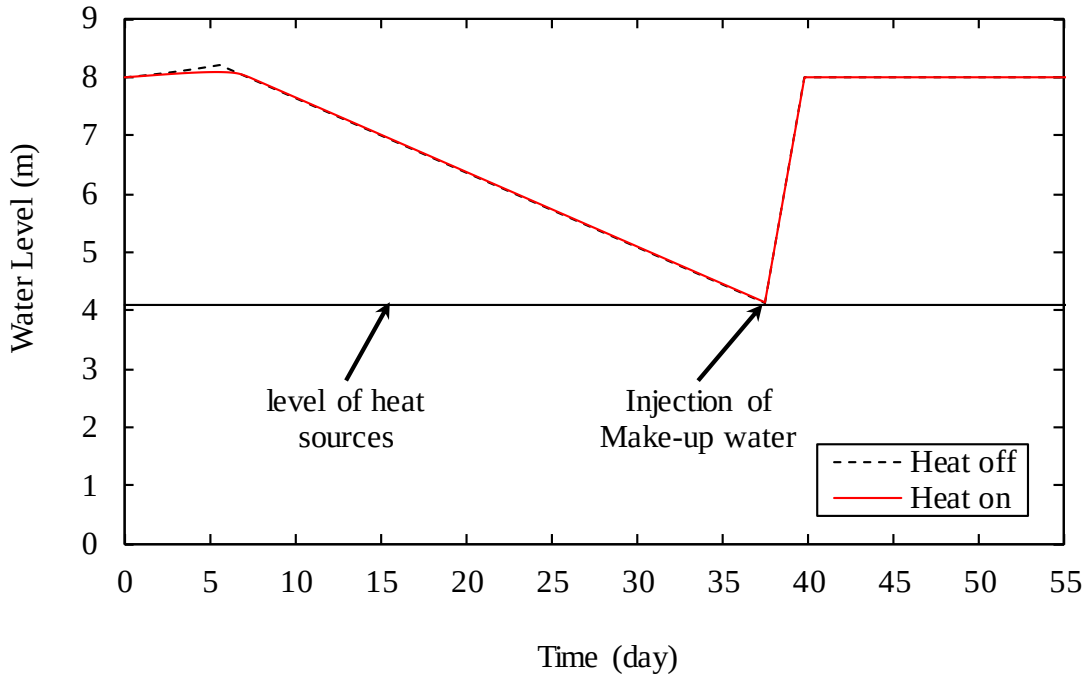

565

566 Figure 11. Water level during the loss of cooling scenario and after injection of make-up water
567 for the large-scale cooling pond.

568 In Figure 12, for the "Heat off" situation, the sensible heating is faster for the high heat load
569 and once the temperature reaches the boiling point, for both heat loads, the curves become
570 parallel to X-axis. It can also be seen that adopting such "Heat off" assumption can significantly
571 overpredicts the water temperature especially for low heat load values. In Figure 12, the
572 difference between the predictions of water temperature using both assumptions is around 48%
573 for a heat load of 0.5 MW, whereas only 18% is observed for the heat load of 2 MW. This
574 implies that the over-prediction is higher for the low heat load. This is due, as discussed before,
575 to the large exposed area of the water surface to the ambient air, which increases the surface
576 heat loss. Hence, such an assumption should be carefully considered while performing the
577 analysis of accident scenarios for large-scale cooling ponds.

578

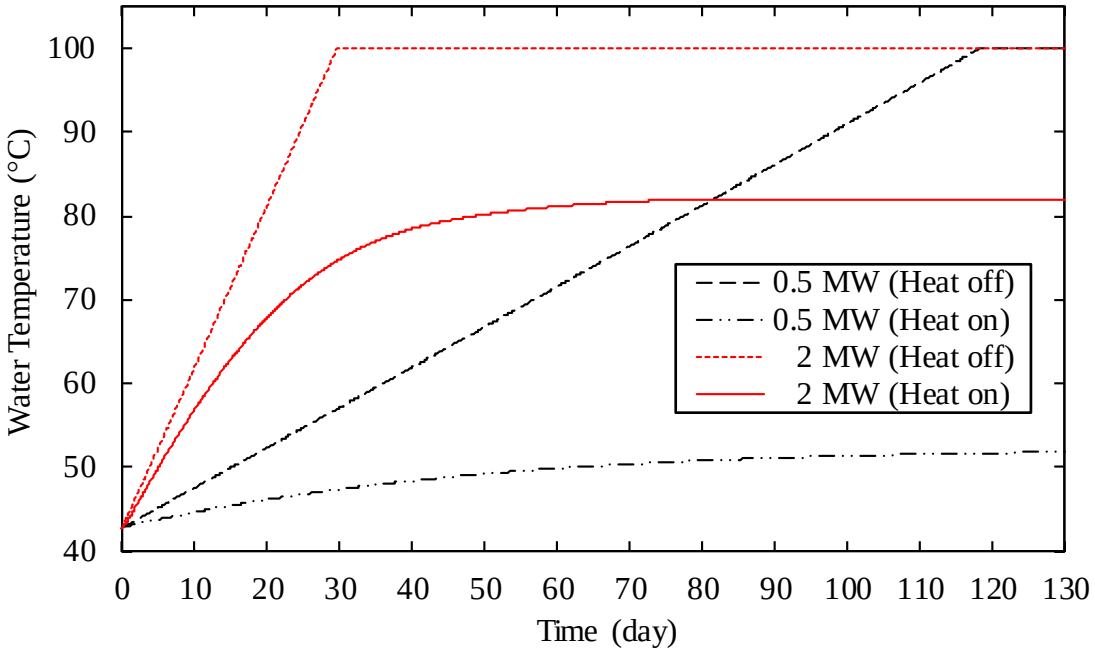

Figure 12. Water temperature under different heat loads for the large-scale cooling pond.

5.3 Impact of Weather Conditions

The outside weather conditions are represented in the Z-D model in terms of outside air temperature and relative humidity. Changes in these conditions may have an effect on the cooling performance of the spent pond. To examine the potential effects, we have conducted a sensitivity study by varying the outside air temperature and relative humidity. As can be seen in Figure 13, the outside air temperature has a significant effect on the water temperature. Increasing the outside air temperature by about 10 °C results in an increase in the water temperature by approximately 9 °C. This is because of the make-up water and ventilation air temperatures are mostly determined by the outside temperature. Also, the temperature drop in the cooling tower, as shown in Figure 2, is affected by the conditions outside.

On the other hand, the relative humidity of the outside air does not have a considerable effect, as shown in Figure 14. This may be because of the air change per hour (ACH) for the pond hall is very low for this type of applications, at about 0.333 per hr. Meanwhile, the amount of water vapour emerging from the water surface due to evaporation is high enough to rapidly increase the relative humidity of the moist air within the pond hall.

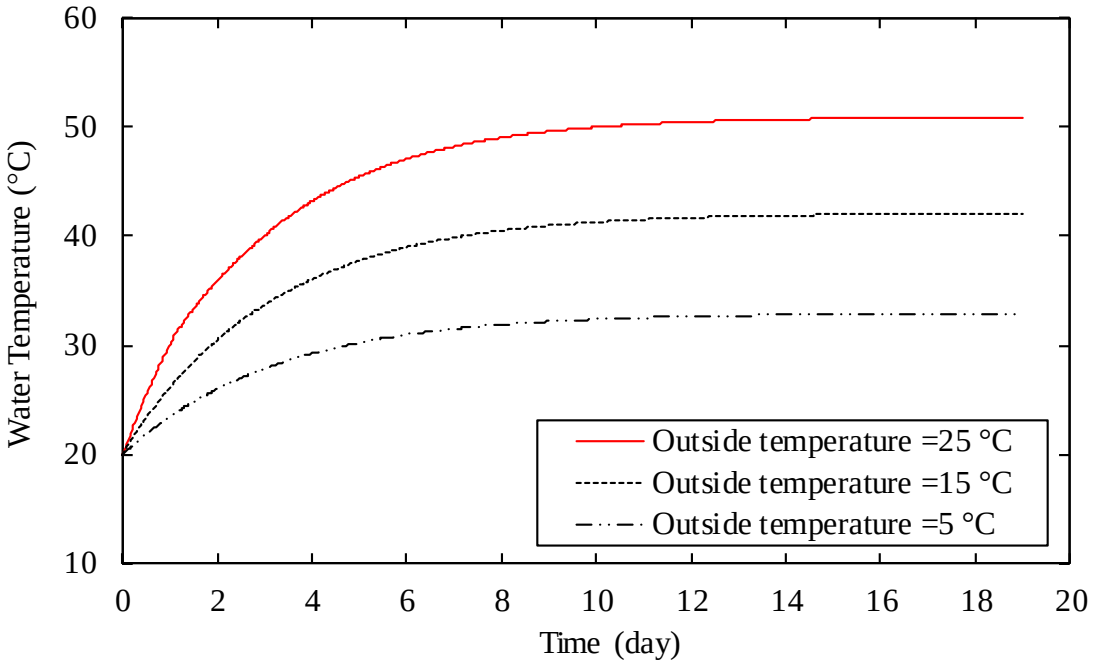

597

598 Figure 13. Effect of outside ambient air temperature on water temperature assuming 0%
599 relative humidity.

600

601

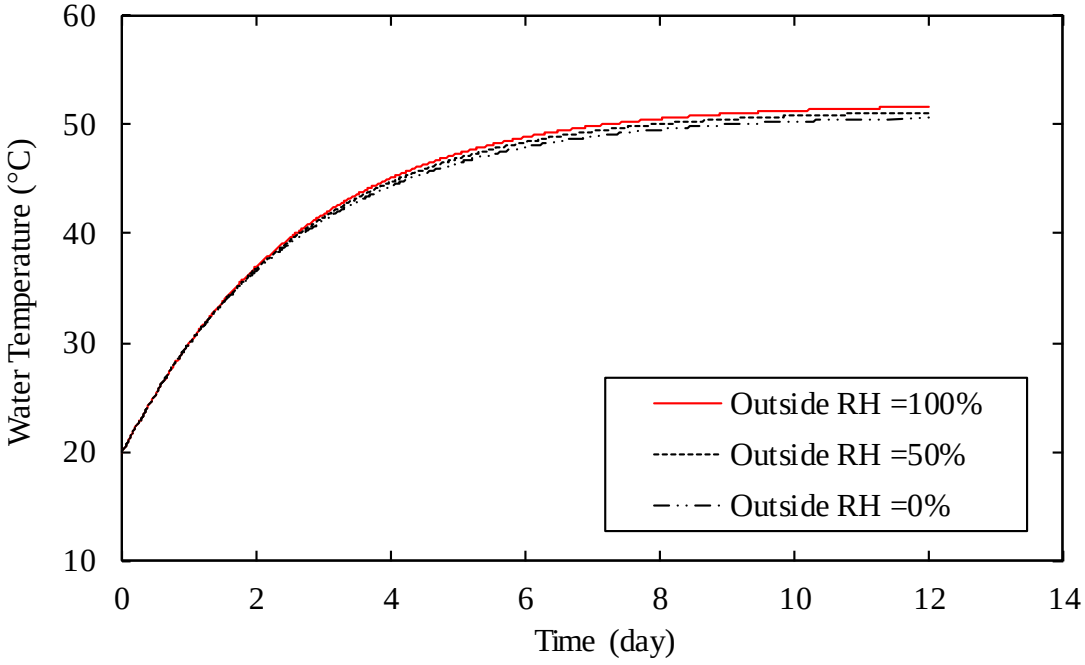

602

603 Figure 14. Effect of the outside relative humidity on water temperature assuming an air
604 temperature of 25 °C.

6 Conclusion

A Z-D model has been developed for large-scale cooling ponds. This model was validated against data reported in the literature for the Maine Yankee spent fuel cooling pond. Also, another validation exercise was performed to examine the applicability of the Z-D model to predict the water temperature for the large-scale cooling pond. However, this validation was limited to low water temperatures where validation with higher water temperatures (near 100 °C) has not been conducted due to the limited data available for the large-scale cooling ponds and the difficulty of producing such data. It can be seen from the validation exercises that the Z-D thermal model is able to predict the thermal behaviour of the cooling ponds under the considered operational scenarios and with various pond sizes.

A number of parametric studies were performed in different situations. The first study concerned the performance of the pond under normal operating conditions where the pond water and air temperatures are evaluated. In the same study, the proportions of heat removal components were quantified. Furthermore, a loss of cooling analysis was conducted under two conditions; one without surface heat transfer and another with heat transfer. It was found that the assumption leading to ignoring the heat loss from the water surface is not always a good choice.

The last study was performed to examine the sensitivity of the pond water temperature to variation in outside weather conditions. The outcomes reveal that water temperature is rather insensitive to the outside relative humidity under the given scenario and the assumption of constant efficiency of the cooling tower, which limits the effect of the relative humidity on the cooling tower performance. On the other hand, relatively high sensitivity was observed to variations in outside temperature. However, further sensitivity studies are needed to determine the effect of the input parameters on the Z-D model's predictions. These studies can be conducted using an appropriate statistical method in combination with the Z-D model. The Z-D model will allow many studies to be performed within a reasonable time. In order to improve the Z-D model, a full description of the cooling tower process need to be included.

References

[1] B. Zohuri and N. Fathi, *Thermal-hydraulic analysis of nuclear reactors*. Springer, 2015.

[2] W. Kuo, G. Yun, and Z. He-yi, "Spent fuel pool transient analysis under accident case and the flow establishment process of passive cooling system," in *Information Systems*

for Crisis Response and Management (ISCRAM), 2011 International Conference on, 2011, pp. 482-491: IEEE.

[3] *UK Government. (September 15, 2016). Government confirms Hinkley Point C project following new agreement in principle with EDF. Accessed 10 Januray 2017*. Available: https://www.gov.uk/government/news/government-confirms-hinkley-point-c-project-following-new-agreement-in-principle-with-edf

[4] Y. V. Kozlov, V. Safutin, N. Tikhonov, A. Tokarenko, and V. Spichev, "Long-term storage and shipment of spent nuclear fuel," *Atomic Energy*, vol. 89, no. 4, pp. 792-803, 2000.

[5] K.-I. Ahn, J.-U. Shin, and W.-T. Kim, "Severe accident analysis of plant-specific spent fuel pool to support a SFP risk and accident management," *Annals of Nuclear Energy*, vol. 89, pp. 70-83, 2016.

[6] Y.-S. Chen and Y.-R. Yuann, "Accident mitigation for spent fuel storage in the upper pool of a Mark III containment," *Annals of Nuclear Energy*, vol. 91, pp. 156-164, 2016.

[7] W. Fu, X. Li, X. Wu, and Z. Zhang, "Investigation of a long term passive cooling system using two-phase thermosyphon loops for the nuclear reactor spent fuel pool," *Annals of Nuclear Energy*, vol. 85, pp. 346-356, 2015.

[8] J. R. Wang, H. T. Lin, Y. S. Tseng, and C. K. Shih, "Application of TRACE and CFD in the spent fuel pool of Chinshan nuclear power plant," in *Applied Mechanics and Materials*, 2012, vol. 145, pp. 78-82: Trans Tech Publ.

[9] S.-i. Tanaka, "Accident at the Fukushima Daiichi nuclear power stations of TEPCO: outline & lessons learned," *Proceedings of the Japan Academy, Series B*, vol. 88, no. 9, pp. 471-484, 2012.

[10] R. Hasan, J. Tudor, and A. Ramadan, "Modelling of flow and heat transfer in spent fuel cooling ponds," in *Proceedings of the International Congress on Advances in Nuclear Power Plants* 2015, Nice, France.

[11] C. Ye, M. Zheng, M. Wang, R. Zhang, and Z. Xiong, "The design and simulation of a new spent fuel pool passive cooling system," *Annals of Nuclear Energy*, vol. 58, pp. 124-131, 2013.

[12] T.-C. Hung, V. K. Dhir, B.-S. Pei, Y.-S. Chen, and F. P. Tsai, "The development of a three-dimensional transient CFD model for predicting cooling ability of spent fuel pools," *Applied Thermal Engineering*, vol. 50, no. 1, pp. 496-504, 2013.

[13] S. Chen, W. Lin, Y. Ferng, C. Chieng, and B. Pei, "Development of 3-D CFD methodology to investigate the transient thermal-hydraulic characteristics of coolant in a spent fuel pool," *Nuclear Engineering and Design*, vol. 275, pp. 272-280, 2014.

[14] C. Yanagi, M. Murase, Y. Yoshida, Y. Utanohara, T. Iwaki, and T. Nagae, "Numerical Simulation of Water Temperature in a Spent Fuel Pit during the Shutdown of Its Cooling Systems," *Journal of Power and Energy Systems*, vol. 6, no. 3, pp. 423-434, 2012.

[15] C. Yanagi, M. Murase, Y. Yoshida, T. Iwaki, T. Nagae, and Y. Koizumi, "Evaporation heat flux from hot water to air flow," *Nippon Kikai Gakkai Ronbunshu, B Hen*, vol. 78, no. 786, pp. 363-372, 2012.

[16] C. Yanagi and M. Murase, "One-Region Model Predicting Water Temperature and Level in a Spent Fuel Pit during Loss of All AC Power Supplies," *Journal of Power and Energy Systems*, vol. 7, no. 1, pp. 18-31, 2013.

[17] C. Yanagi, M. Murase, and Y. Utanohara, "Effects of Decay Heat Distribution on Water Temperature in a Spent Fuel Pit and Prediction Errors With a One-Region Model," *Journal of Nuclear Engineering and Radiation Science*, vol. 2, no. 3, p. 031001, 2016.

[18] S. Carlos, F. Sanchez-Saez, and S. Martorell, "Use of TRACE best estimate code to analyze spent fuel storage pools safety," *Progress in Nuclear Energy*, vol. 77, pp. 224-238, 11// 2014.

[19] V. Ognerubov, A. Kaliatka, and V. Vileiniškis, "Features of modelling of processes in spent fuel pools using various system codes," *Annals of Nuclear Energy*, vol. 72, pp. 497-506, 2014.

[20] P. Groudev, A. Stefanova, and M. Manolov, "Investigation of dry out of SFP for VVER440/V230 at Kozloduy NPP," *Nuclear Engineering and Design*, vol. 262, pp. 285-293, 2013.

[21] A. Kaliatka, V. Ognerubov, and V. Vileiniskis, "Analysis of the processes in spent fuel pools of Ignalina NPP in case of loss of heat removal," *Nuclear Engineering and Design*, vol. 240, no. 5, pp. 1073-1082, 2010.

[22] T. Watanabe, M. Ishigaki, and M. Hirano, "Analysis of BWR long-term station blackout accident using TRAC-BF1," *Annals of Nuclear Energy*, vol. 49, pp. 223-226, 2012.

[23] X. Wu, W. Li, Y. Zhang, W. Tian, G. Su, and S. Qiu, "Analysis of the loss of pool cooling accident in a PWR spent fuel pool with MAAP5," *Annals of Nuclear Energy*, vol. 72, pp. 198-213, 2014.

[24] C. M. Lee and K. Lee, "A study on operation time periods of spent fuel interim storage facilities in South Korea," *Progress in Nuclear Energy*, vol. 49, no. 4, pp. 323-333, 2007.

[25] K. A. Rogers, "Fire in the hole: A review of national spent nuclear fuel disposal policy," *Progress in Nuclear Energy*, vol. 51, no. 2, pp. 281-289, 2009.

[26] C. B. Keil, C. E. Simmons, and T. R. Anthony, *Mathematical Models for Estimating Occupational Exposure to Chemicals*. American Industrial Hygiene Association, 2009.

[27] R. J. LeVeque, *Finite difference methods for ordinary and partial differential equations: steady-state and time-dependent problems*. Siam, 2007.

[28] Y. Cengel, *Heat Transfer A Practical Approach, McGraw-Hill*, 2 ed. (Ellison, New York). 2003, p. 609.

[29] A. C. Yunus and A. B. Michael, "Thermodynamics: An engineering approach," *McGraw-Hill, New York*, 2006.

[30] J. D. Hoffman and S. Frankel, *Numerical methods for engineers and scientists*. CRC press, 2001.

[31] T. George, S. Claybrook, L. Wiles, and C. Wheeler, "GOTHIC Containment Analysis Package, User Manual, Version 7.2 b, NAI 8907-02 Rev 18," 2009.